

Reverse anionic flotation of dolomitic collophanite using a mixed fatty acid collector: Adsorption behavior and mechanism

Wei Xu ^{1,2,3}, Qun Liang ¹, Yan Tian ^{2,3}, Guangjun Mei ^{1,2,3}

¹School of Resources and Environmental Engineering, Wuhan University of Technology, Wuhan, 430070, China

²State Key Laboratory of Mineral Processing, Beijing, 102628, China

³State Key Laboratory of Efficient Utilization for Low Grade Phosphate Rock and Its Associated Resources, Guiyang, 550002, China

Corresponding author: meijuangjun@whut.edu.cn (Guangjun Mei)

Abstract: Collophanite in south China generally has a high MgO level, which negatively impacts wet-process phosphoric acid production and cannot be utilized directly. A novel mixed fatty acid soap (GSWF01) was employed as a collector for dolomite. A single reverse flotation experiment was performed on a dolomitic collophanite from Guizhou, China under different pH and collector dosages. A phosphate concentrate with P₂O₅ grade of 33.73%, MgO content of 1.07%, MER value ($\omega(\text{MgO}+\text{Al}_2\text{O}_3+\text{Fe}_2\text{O}_3)/\omega(\text{P}_2\text{O}_5)$) of 4.86% and phosphorus recovery of 91.06% was obtained. The beneficiation indexes of GSWF01 were better than that of sodium oleate (NaOL). The adsorption behavior and mechanism of GSWF01 on dolomite surface were investigated using quartz crystal microbalance with dissipation (QCM-D), atomic force microscope (AFM), infrared spectrometer (IR), and zeta potentiometer. The results revealed that GSWF01 chemically reacted with metal ions (Ca²⁺, Mg²⁺, etc.) on the surface of dolomite to generate fatty acid salt precipitation (chemisorption). The adsorbed layer transitioned from dense to loose in two stages, resulting in a stable double-layer adsorption structure. Moreover, in a weak acidic solution environment, physical adsorption of fatty acid molecules (RCOOH (aq)) and fatty acid ion-molecular association compounds (RCOOH · RCOO⁻) generated by hydrolysis can also occur on the dolomite surface. These are the main reasons for the hydrophobic floating of dolomite. This is of great significance to the development of a novel high-efficiency dolomite collector and the enhancement of flotation process for carbonate collophanite.

Keywords: collophanite, anionic collector, dolomite, QCM-D, adsorption mechanism

1. Introduction

Phosphate ore, an irreplaceable and non-renewable strategic mineral resource, is the primary raw material for wet-process phosphoric acid and its deep processing, which is critical for developing the phosphorus chemical industry. China has the world's second-largest phosphate resource. However, most of them are concentrated as collophanite in southern China (e.g., Yunnan, Guizhou, Hubei, Sichuan, Hunan, etc.), and cannot be directly utilized without beneficiation (Deng et al. 2020; Derhy et al. 2020). Collophanite generally has a high MgO content, which has adverse effects on the processing and production of downstream wet-process phosphoric acid and phosphate compound fertilizer, such as increasing acid consumption, aggravating equipment corrosion, low P₂O₅ conversion rate, poor product quality, etc. (Xu et al. 2021). Currently, China phosphorus chemical industries require P₂O₅ grade greater than 32%, MgO content less than 1.2%, and MER value ($\omega(\text{MgO} + \text{Al}_2\text{O}_3 + \text{Fe}_2\text{O}_3)/\omega(\text{P}_2\text{O}_5)$) less than 8.5% for phosphate concentrate used for wet-process.

The most effective method for removing magnesium impurities from phosphate ore is reverse flotation. It is a relatively mature beneficiation process adopted by most phosphate ore concentrators in the world (Ruan et al. 2019). The reverse flotation removal of magnesium-bearing minerals is generally carried out in a weakly acidic solution with an anionic collector. Generally, long-chain fatty acids and their salts are the main carbonate mineral collectors (Liu et al. 2017; Xu et al. 2012; Shi et al. 2021; Ruan

et al. 2017). In recent years, in order to explore properties of fatty acid collectors, most traditional non-real-time or non-in-situ testing methods, such as zeta potentiometer, contact angle measuring instrument, infrared spectroscopy (IR), scanning electron microscopy (SEM), X-ray photoelectron spectroscopy (XPS), etc., have been widely utilized to investigate the flotation adsorption behavior, particularly in the study of reagent action rules (Qi and Sun 2013; Ruan et al. 2018; Yu et al. 2016). Although previous research results have enriched the basic theory of flotation application, the innovative development of adsorption theory remains lagging due to research methods' limitations, which restricts the rapid development and application of new efficient anionic collector products.

Quartz crystal microbalance with dissipation (QCM-D) is precision equipment used to study the surface interaction process and surface quality change (Kou et al. 2016). Its most notable feature is its ability to measure the amount and process of material adsorption on a specific surface in real-time in a liquid environment. Meanwhile, the viscoelastic modulus of adsorbed layer can also be obtained, and structural changes in the adsorbed layer can be predicted, which compensates for the shortcomings of traditional research methods. Teng et al. (2012) used QCM-D to study the entire isopentyl xanthate adsorption and desorption process on the surface of ZnS resonator activated by Ag^+ , obtaining real-time information on adsorption and conformational changes of adsorbed layer. Deng et al. (2013) used QCM-D to prove that gypsum precipitates on SiO_2 and ZnS surfaces and that the interaction of gypsum particles with SiO_2 and ZnS resonators is reversible physical adsorption. Kou et al. (2010a and 2010b) used QCM-D to study the dynamic adsorption of cationic amine collectors on quartz surface and anionic fatty acid collectors on phosphate mineral surface and obtained appropriate adsorption dynamic properties. Therefore, QCM-D provides a novel research method for exploring the mechanism of flotation reagents.

In the current study, a dolomitic collophanite ore from Guizhou, China, was taken as the research object. A novel and efficient mixed fatty acid soap (GSWF01) was utilized as the dolomite collector. A single reverse flotation process in a weak acid solution system produced excellent beneficiation indexes. Subsequently, the adsorption behavior and mechanism of GSWF01 on dolomite surface were explored for the first time using QCM-D combined with atomic force microscope (AFM), infrared spectrometer (IR), and zeta potentiometer, and adsorption kinetic property information was obtained. The results further explain the essence of selective adsorption of fatty acid collectors on the dolomite surface and supplement the basic theory of reverse anionic flotation application. This has practical implications for modifying and developing new magnesium removal collectors.

2. Materials and methods

2.1. Selected ore sample

A phosphate mining enterprise in Guizhou, China, provided massive phosphorite. After mechanical crushing and grinding, raw ore powder with a particle size fraction of $-75 \mu\text{m}$ was obtained, accounting for 57.90% of the total for flotation. Table 1 shows the chemical analysis results of raw ore products with different grain sizes after wet screening using an X-ray fluorescence spectrometer (XRF) (model AxiosmAX, PANalytical B.V., The Netherlands). The phase identification of raw ore and pure mineral powder was carried out using an X-ray diffractometer (XRD) (model X'Pert3 Powder, PANalytical B.V., The Netherlands) (Fig. 1a). For scanning the elemental mapping distribution of $-38 \mu\text{m}$ raw ore, a scanning electron microscope (SEM) (model EVO 15, Carl Zeiss Corporation, Germany) and energy dispersive X-ray spectrometer (EDS) (model INCA X-act, Oxford Instruments Corporation, UK) were used, as displayed in Fig. 2. The results demonstrated that element P was found mostly in fluorapatite (the target mineral), while Mg and Si occurred in dolomite and quartz, respectively (Figs. 1a and 2). Mineral particles were irregular in shape (mainly granular and massive) and had uneven particle size distribution. $-38 \mu\text{m}$ fine particles accounted for 36.08%, indicating an obvious trend of fine particle enrichment (Table 1). A portion of fluorapatite was found closely associated with gangue minerals (dolomite, quartz, etc.), presenting the characteristics of fine-grained collophanite (Fig. 2). The ore, with P_2O_5 grade of 27.67%, $\omega(\text{CaO})/\omega(\text{P}_2\text{O}_5)$ value of 1.56, MgO content of 4.72% ($> 1.20\%$, the main harmful metal impurity), sesquioxide ($\text{Al}_2\text{O}_3+\text{Fe}_2\text{O}_3$) content of 0.41%, and MER value ($\omega(\text{MgO}+\text{Al}_2\text{O}_3+\text{Fe}_2\text{O}_3)/\omega(\text{P}_2\text{O}_5)$) of 18.54% (Table 1), cannot be used directly in the production of downstream phosphoric acid and fertilizer products. As observed, the ore was fine-grained dolomitic

collophanite with a high grade and low sesquioxide content. Dolomite removal can reduce the MER value in the ore.

Table 1. Chemical element analysis and distribution rate of raw ore products with different grain sizes

Particle size (μm)	Yield (wt. %)	Grade (wt. %)						Distribution rate (wt. %)					
		P ₂ O ₅	MgO	CaO	SiO ₂	Al ₂ O ₃	Fe ₂ O ₃	P ₂ O ₅	MgO	CaO	SiO ₂	Al ₂ O ₃	Fe ₂ O ₃
+75	42.1	27.10	4.47	42.22	13.15	0.04	0.19	41.23	39.92	41.13	52.74	12.95	28.57
38–75	21.82	27.63	5.06	43.45	9.63	0.03	0.25	21.79	23.39	21.94	20.01	5.04	19.48
–38	36.08	28.36	4.80	44.24	7.93	0.30	0.40	36.98	36.69	36.93	27.25	82.01	51.95
Total	100	27.67	4.72	43.22	10.50	0.13	0.28	100.00	100.00	100.00	100.00	100.00	100.00

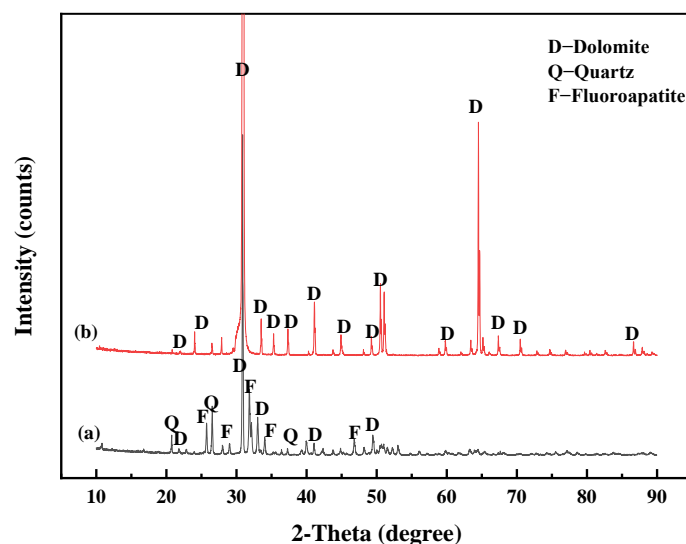


Fig. 1. XRD patterns of selected raw ore and pure mineral dolomite: (a) Collophanite; (b) Dolomite

2.2. Pure mineral

Natural granular dolomite, provided by a mineral specimen firm in Guangzhou, China, was mechanically ground and sent to an X-ray powder diffractometer (XRD) (model X'Pert3 Powder, PANalytical B.V., the Netherlands) and a laser granulometer (model MS3000+LV, Malvern Instruments Co. Ltd., UK) for purity and particle size analysis. The results showed no obvious impurities in the dolomite powder, with high purity ($> 98\%$) (Fig. 1b) and fine particle size distribution ($D_v(50) = 3.38 \mu\text{m}$), meeting the requirements of zeta potential and IR test.

2.3. Flotation reagents

WFS, an industrial chemical wastewater ($\text{pH} = 1 - 2$) from Wengfu (Group) Co. Ltd., China, was used as pH regulator and inhibitor, mainly composed of sulfuric acid and phosphoric acid. GSWF01, a mixture of fatty acid soaps with different carbon chain lengths, was employed as a collector for dolomite. It was an independent research and development product supplied by State Key Laboratory of Efficient Utilization for Low Grade Phosphate Rock and Its Associated Resources, China, and configured as 1% aqueous solution for use. Sodium oleate (NaOL) (chemically pure, Shanghai Zhanyun Chemical Co. Ltd., China) was used a reference collector in 1% aqueous solution.

2.4. Flotation experiments

A total of 150 g raw ore was loaded into a 0.5 dm³ single cell flotation machine (model RK/FD III, Wuhan Rock Grinding Equipment Co. Ltd., China), and the initial parameters of the flotation machine were set to 25% pulp mass fraction, 1900 r/min rotation speed and 20 °C pulp temperature. WFS, an acid inhibitor, was first added to adjust the pH of the pulp, followed by dolomite collector GSWF01 addition. After stirring for 2 min, the air was introduced, and froth were scraped for 2.5 min. The froth

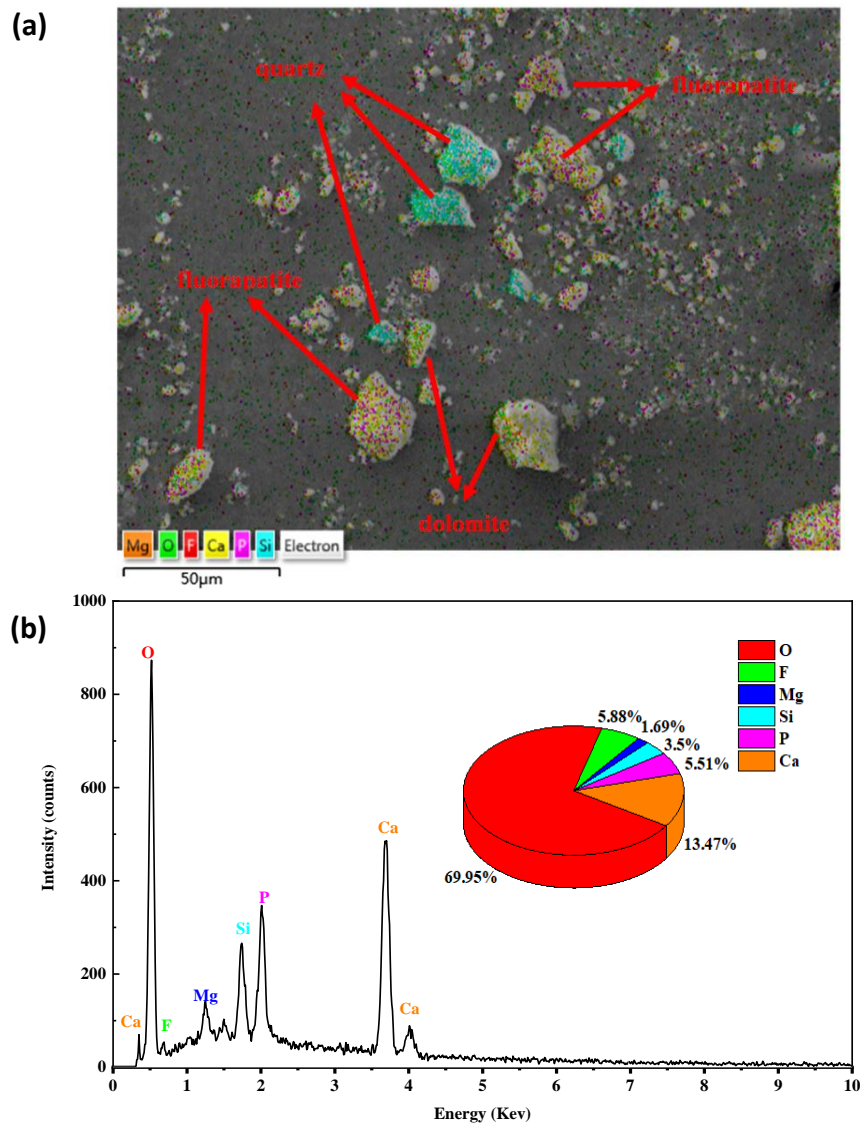


Fig. 2. SEM-EDS surface distribution of raw ore with the particle size of $-38 \mu\text{m}$: (a) EDS Layered Image ; (b) Energy spectrum and element distribution diagram

product was as reverse flotation tailings, while the sink was as reverse flotation concentrate. The two products were dried, weighed, mixed, divided, and sampled. The yield and recovery were calculated after analysis of each element.

2.5. QCM-D analyses

The adsorption kinetics of the collector on the mineral surface was studied using a quartz crystal microbalance with dissipation (QCM-D) (model Q-Sense Explorer, Biolin Scientific, Sweden) ((Kou et al. 2010; Sedeva et al. 2010). The QCM-D is a real-time analysis apparatus for molecular interaction at the solid-liquid interface, and its main working units are depicted in Fig. 3. The core component of QCM-D quartz crystal resonator is composed of an AT cut quartz crystal sandwiched between two gold electrodes. Different substances can be cladded or modified on the working electrode's surface. In this study, the cladding material used is dolomite ($\text{CaMg}(\text{CO}_3)_2$). QCM-D can simultaneously detect variation in resonance frequency (Δf) and change in energy dissipation (ΔD) caused by adsorption or de-adsorption of reagent molecules on the resonator surface (Gutig et al. 2008; Paul et al. 2008). A fresh, vacuum-sealed, custom-made quartz crystal sensor with dolomite coating (QSX 999, Biolin Scientific, Sweden) was installed in the QCM-D flow cell and was first measured in an air medium during the test. After Δf and ΔD signals were stabilized, ultrapure water was pumped until adsorption equilibrium.

The collector solution to be measured (concentration, 10 mmol/dm³) was pumped into the system once Δf and ΔD signals were stabilized again, and the collector began to adsorb on the dolomite surface. The experiment ended after the adsorption reached equilibrium again. The solution temperature was controlled at 25 ± 0.05 °C throughout the experiment. After testing, Qsense Dfind software was used to fit the quality and viscoelastic data of the adsorbed layer on the dolomite surface.

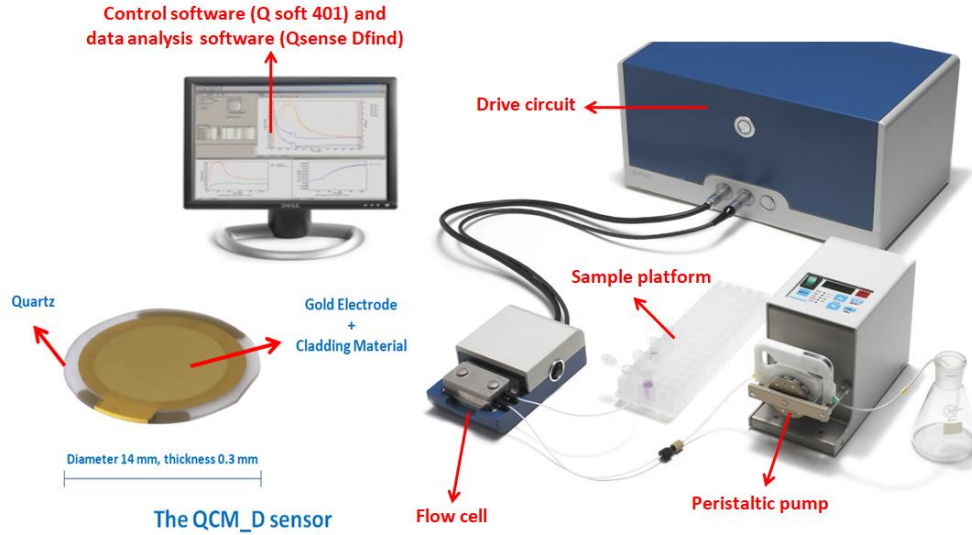


Fig. 3. Main working units of QCM-D

When the adsorbed layer is thin and firmly adsorbed ($\Delta D < 1 \times 10^{-6}$), according to Sauerbrey equation (Sauerbrey 1959) (Eq. (1)), Δf is proportional to Δm , and Δm can be calculated from the measured Δf . When the adsorption amount of reagent on the surface of the resonator is large, the multilayer adsorption is formed, and the adsorbed layer cannot be fully coupled with the resonator surface, resulting in a high system dissipation ($\Delta D \geq 1 \times 10^{-6}$). In this case, the Voigt model (Voinova et al. 1998; Vogt et al. 2004) (Eqs. (2) and (3)) can be used to fit the quality and properties of the adsorbed layer.

$$\Delta m = -\frac{\rho_q t_q \Delta f}{f_0 n} = -\frac{\rho_q v_q \Delta f}{2 f_0^2 n} = -\frac{C \Delta f}{n} \quad (1)$$

In Eq. (1), C is a constant with a value of $17.8 \text{ ng} \cdot \text{cm}^{-2} \cdot \text{Hz}^{-1}$. N is the harmonic number, when $n=1$, $f = f_0 = 5 \text{ MHz}$, where f_0 is the fundamental frequency, and ρ_q , t_q and v_q are the density, time, and viscoelasticity of the adsorbed layer, respectively when the adsorption equilibrium is achieved.

$$\Delta f \approx -\frac{1}{2\pi\rho_0 h_0} \left\{ \frac{\eta_3}{\delta_3} + \sum_{j=1,2} \left[\rho_j \omega - 2h_j \left(\frac{\eta_3}{\delta_3} \right)^2 \frac{\eta_j \omega^2}{\mu_j^2 + \eta_j^2 \omega^2} \right] \right\} \quad (2)$$

$$\Delta D \approx -\frac{1}{2\pi f \rho_0 h_0} \left\{ \frac{\eta_3}{\delta_3} + \sum_{j=1,2} \left[2h_j \left(\frac{\eta_3}{\delta_3} \right)^2 \frac{\mu_j \omega^2}{\mu_j^2 + \eta_j^2 \omega^2} \right] \right\} \quad (3)$$

In Eqs. (2) and (3), ρ , h , μ , η , δ and ω are the density, thickness, shear elastic modulus, shear viscosity, shear wave penetration depth, and angular frequency of the adsorbed layer, respectively.

2.6. AFM characterization

An atomic force microscope (AFM) (model MFP-3D Origin, Asylum Research, USA) was used to study the surface morphology of the dolomite-coated resonator before and after GSWF01 adsorption. The test samples were a clean dolomite-coated resonator and a naturally dried resonator after QCM-D adsorption equilibrium, respectively. The silicon probe model TSAC240-R3 with a fundamental frequency of 70 kHz and a force constant of 2 N/m was selected. The sample surface was scanned in tapping mode and at room temperature during the test. The original 2D and 3D surface morphology were analyzed by Igor Pro 6.37 software.

2.7. FTIR analysis

A total of 2.5 g dolomite powder was added in a 100 cm³ beaker, followed by 50 cm³ ultrapure water and a sufficient amount of GSWF01 collector (6 mmol/dm³), and the mixture was stirred for 0.5 h to allow the reagent and mineral to interact under natural pH conditions thoroughly. The supernatant was poured out after natural settlement. The dolomite precipitates were obtained using vacuum extraction and filtration. The samples were washed three times and dried naturally at room temperature. For FTIR analysis, 25 mg dry sample was mixed with a moderate amount of potassium bromide (KBr) and ground to a fineness of -0.1 mm. After tablet pressing, the sample was determined using a Fourier transform infrared spectrometer (model iCAN9, Tianjin Energy Spectrum Technology Co. Ltd., China). In addition, single dolomite powder and collector were also characterized by infrared spectroscopy for reference.

2.8. Zeta potential measurements

In a 100 cm³ beaker, 50 mg dolomite powder was added, followed by a 50 cm³ potassium nitrate (KNO₃) auxiliary electrolyte solution (1 mmol/dm³), and ultrasonic dispersion was performed for 5 min. The pH range of the solution was adjusted using hydrochloric acid (HCl) or sodium hydroxide (NaOH), followed by the addition of an appropriate amount of GSWF01 collector (6 mmol/dm³) (for single mineral measurements, the same amount of ultrapure water was added). After stirring for 2 min, the pH value was measured and recorded. After standing, the upper suspension was injected into the electrophoresis cell of the zeta electrophoresis apparatus (model JS94H, Shanghai Zhongchen Digital Technic Apparatus Co. Ltd., China) for potential measurement. Each sample was measured three times, and the average value was reported. All solution tests were carried out in ultrapure water and at room temperature.

3. Results and discussion

3.1. Flotation experiments

3.1.1. Effect of pH

Magnesium removal by reverse flotation is usually achieved in weak acid solution, and acid inhibitors play a significant role in the selective enhanced separation of apatite and dolomite (Zou et al. 2019; Liu et al. 2017a; Liu et al. 2017b). WFS, a mixed acid mainly composed of sulfuric acid and phosphoric acid, was used as a combination inhibitor to carry out reverse flotation tests of acidic pulp at different pH values, as illustrated in Fig. 4. P₂O₅ grade and MgO removal in phosphate concentrate (i.e., MgO recovery of flotation tailings) increased with an increase in pH, while P₂O₅ recovery and MgO content of phosphate concentrate declined, indicating a trend of ebb and flow. On balance, when pH value was 5, the quality of phosphate concentrate and P₂O₅ recovery were relatively superior, which can be used as an appropriate pH choice. According to Li and Tian (2016), the flotation effect of mixed acid containing sulfuric acid and phosphoric acid as an inhibitor is better than that of single acid. The H⁺ electrolyzed by mixed acid can react with HCO₃⁻ and CO₃⁻ to reduce the concentration of anions on the mineral surface, and the generated CO₂ can inhibit the formation of hydrogen bonds on the surface of dolomite minerals, thus enhancing the dolomite surface activity. Furthermore, H₂PO₄⁻, HPO₄²⁻ and PO₄³⁻ formed by mixed acid ionization easily adsorbed on the surface of apatite, forming competitive adsorption with fatty acid radicals and inhibiting apatite floating, thus achieving differential flotation separation of dolomite and apatite.

3.1.2. Effect of collector dosage

The type and dosage of the collector in a phosphate ore reverse flotation system directly affect the flotation index (Derhy et al. 2020). GSWF01, a novel mixed fatty acid soap, was used as a collector for dolomite flotation, and reverse flotation experiments were performed at different collector dosages, as shown in Fig. 5. With the increase of collector dosage, P₂O₅ grade and MgO removal in phosphate concentrate (i.e., MgO recovery of flotation tailings) increased continuously, while P₂O₅ recovery and MgO content of phosphate concentrate decreased continuously. Comprehensively considered, when

the dosage of GSWF01 was 0.40 kg/Mg and pH value was 5, the quality of phosphate concentrate and P_2O_5 recovery (P_2O_5 grade of 33.73%, MgO content of 1.07%, MER value ($\omega(\text{MgO} + \text{Al}_2\text{O}_3 + \text{Fe}_2\text{O}_3)/\omega(\text{P}_2\text{O}_5)$) of 4.86% and recovery of 91.06%) were the best, reaching the requirements of wet-process phosphoric acid production.

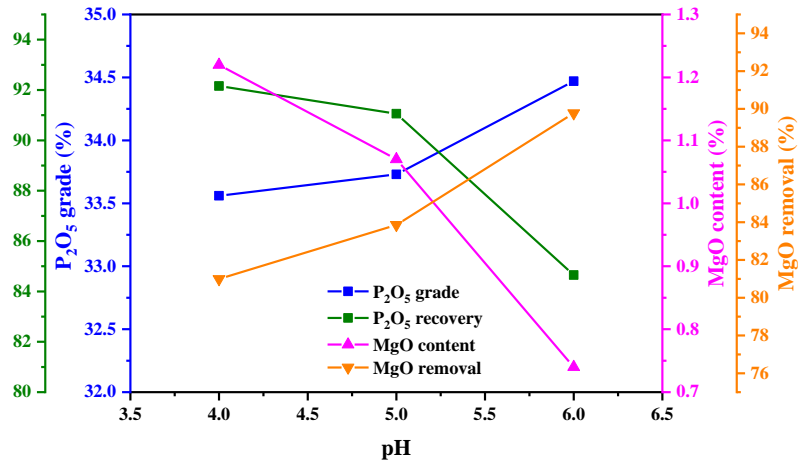


Fig. 4. Effect of pH on phosphate concentrate index (dosage of collector at 0.4 kg/Mg)

3.1.2. Effect of collector dosage

The type and dosage of the collector in a phosphate ore reverse flotation system directly affect the flotation index (Derhy et al. 2020). GSWF01, a novel mixed fatty acid soap, was used as a collector for dolomite flotation, and reverse flotation experiments were performed at different collector dosages, as shown in Fig. 5. With the increase of collector dosage, P_2O_5 grade and MgO removal in phosphate concentrate (i.e., MgO recovery of flotation tailings) increased continuously, while P_2O_5 recovery and MgO content of phosphate concentrate decreased continuously. Comprehensively considered, when the dosage of GSWF01 was 0.40 kg/Mg and pH value was 5, the quality of phosphate concentrate and P_2O_5 recovery (P_2O_5 grade of 33.73%, MgO content of 1.07%, MER value ($\omega(\text{MgO} + \text{Al}_2\text{O}_3 + \text{Fe}_2\text{O}_3)/\omega(\text{P}_2\text{O}_5)$) of 4.86% and recovery of 91.06%) were the best, reaching the requirements of wet-process phosphoric acid production.

Furthermore, the results from XRD in Figs. 6 and 7 display the mineral phases and elements surface distribution in phosphate concentrate and flotation tailings, respectively. Compared with the raw ore, most of the fluorapatite was concentrated in the phosphate concentrate, with only a low content of dolomite (Figs. 6a and 7a). However, a large amount of dolomite was enriched in flotation tailings, accompanied by a small amount of fluorapatite (Figs. 6b and 7b), showing an obvious differentiated enrichment trend. This indicates that the selective separation of dolomite from apatite can be well realized by using GSWF01 collector in weak acidic solution environment.

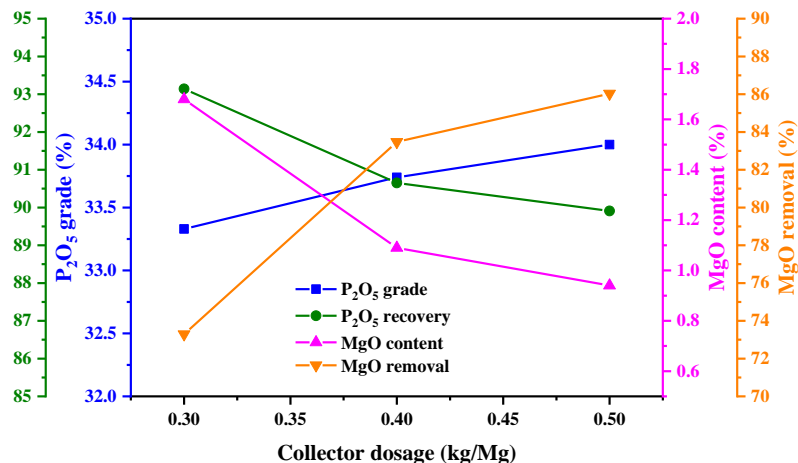


Fig. 5. Effect of collector GSWF01 dosage on phosphate concentrate index (pulp pH = 5)

3.1.3. Performance comparison of GSWF01 and NaOL

In order to better demonstrate the superiority of GSWF-01, NaOL was used as a reference dolomite collector under identical flotation conditions. Fig. 8 displays that the collection performance of mixed fatty acid soap (GSWF01) was significantly better than that of single sodium oleate (NaOL), and the phosphate concentrate quality of the latter cannot meet the requirements of wet-process phosphoric acid production. As a result, GSWF01 was more suitable for the complex flotation practice of phosphate ore than NaOL, while single component NaOL was difficult to realize. This is analogous to the results of Cao et al. (2015). For complex and refractory phosphate ores, obtaining the ideal indicators in beneficiation with a single fatty acid is challenging. However, combining different fatty acids can improve flotation performance (e.g., faster flotation rate, higher recovery, a lower dosage of reagents, etc.).

3.2. Adsorption behavior and mechanism of collector GSWF01 on dolomite surface

To further explain the adsorption behavior and mechanism of GSWF01 on dolomite surface, a highly sensitive in-situ characterization technique QCM-D was employed in conjunction with atomic force microscope (AFM), infrared spectrum (IR), and zeta potential.

3.2.1. QCM-D measurements

To investigate the adsorption characteristics of GSWF01, QCM-D was used to perform real-time and in-situ measurements of the entire process of GSWF01 adsorption on dolomite surface, as shown in Fig. 9. During 0–370 s, ultrapure water, which is more pure than deionized water with a resistivity of 18.2 M Ω ·cm (25°C), was channeled. At this stage, Δf and ΔD are 0, indicating no mass change on the dolomite

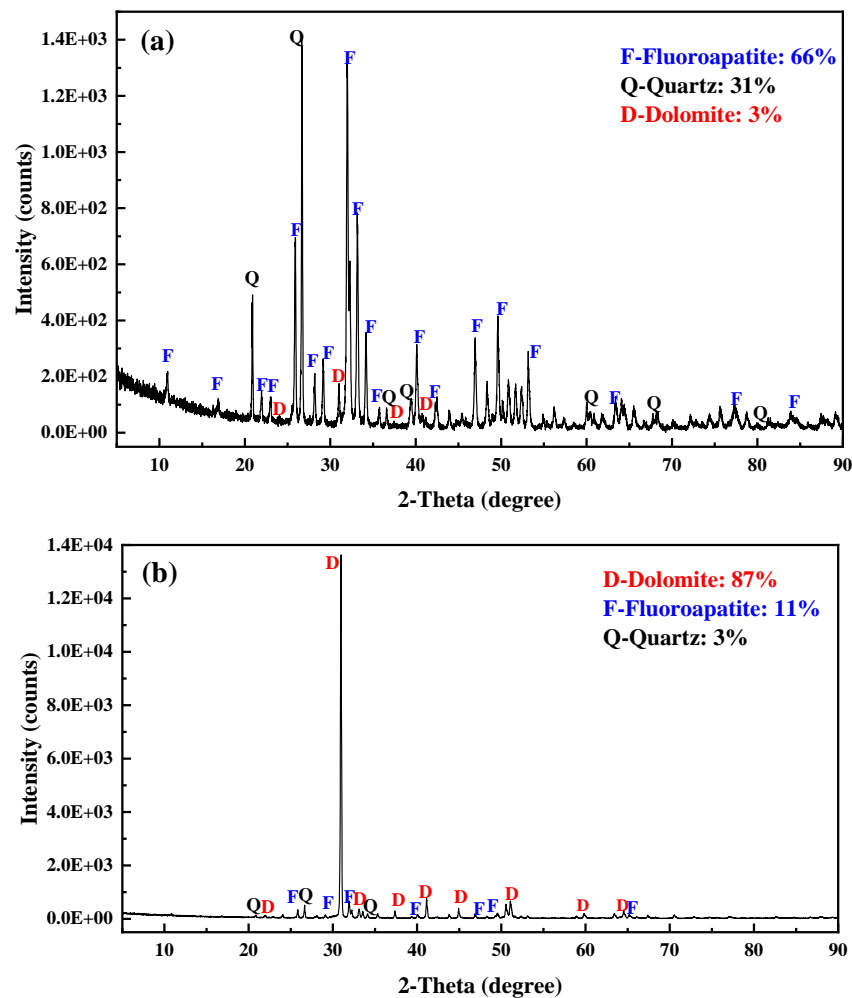


Fig. 6. XRD patterns of ore powder products: (a) phosphate concentrate; (b) magnesium tailings

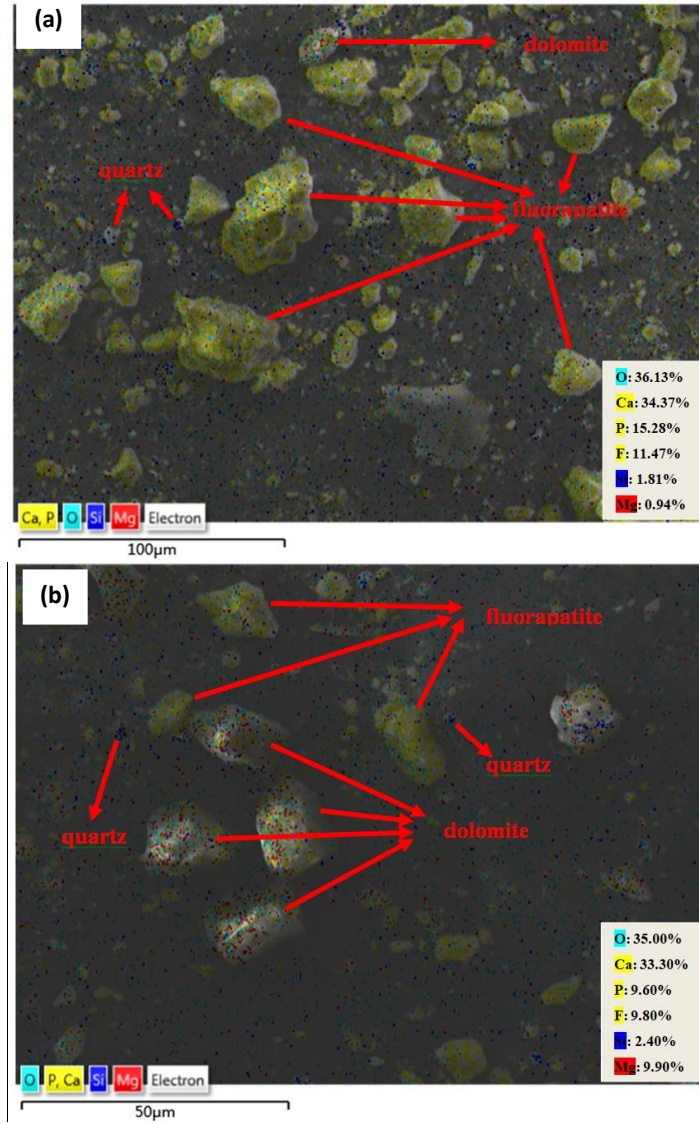


Fig. 7. SEM-EDS surface distribution of elements in ore powder: (a) phosphate concentrate; (b) magnesium tailings

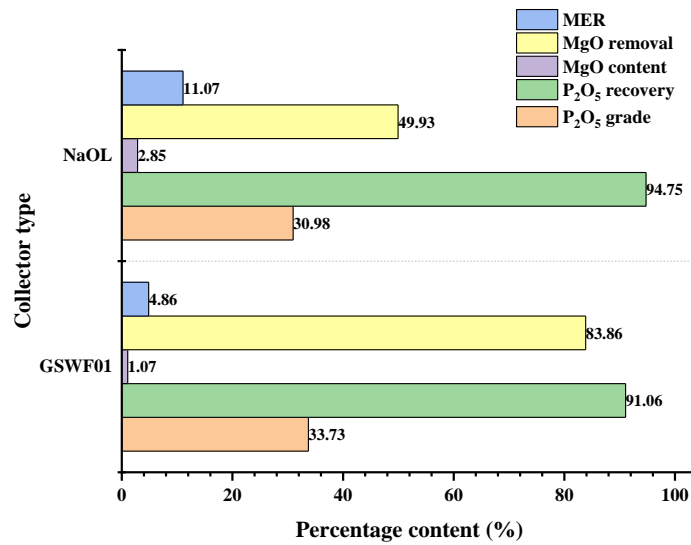


Fig. 8. Comparison of flotation effect between GSWF01 and NaOL (pulp pH = 5, collector dosage of 0.40 kg/t)

surface. Arrow a indicates the beginning of injection of GSWF01 solution into the system. Throughout the adsorption process, Δf dropped rapidly to the lowest point (arrow b, $\Delta f = -10.85$ Hz), then rose to the highest point (arrow c, $\Delta f = -8.34$ Hz), and finally dropped slowly until adsorption equilibrium (arrow f, $\Delta f = -9.58$ Hz), showing an apparent change in adsorption mass on the dolomite surface. However, ΔD immediately rose to the highest point (arrow d, $\Delta D = 1.32 \times 10^{-6}$), then rapidly decreased to the lowest point (arrow e, $\Delta D = 0.96 \times 10^{-6}$), and finally slowly rose until the adsorption equilibrium (arrow g, $\Delta D = 1.33 \times 10^{-6}$), revealing the structural change of the adsorbed layer on the dolomite surface. During 1820–3340 s, the adsorbed layer inclined to be stable, with $\Delta D > 1.0 \times 10^{-6}$, indicating that GSWF01 adsorbed layer on the dolomite surface was viscoelastic with a relatively loose structure. The variation curve of adsorbed layer mass with time was calculated using the Voight model, as displayed in Fig. 10. After injecting the collector solution for 1450 s, an adsorption layer with a mass of 1250 ng/cm² formed on the dolomite surface, and the adsorbed layer mass did not change with the continued solution penetration. In general, the adsorption of fatty acid collector GSWF-01 on dolomite surface is a rapid and stable process, and the viscoelastic hydrophobic adsorption layer formed will not desorbed with an increase of collector concentration.

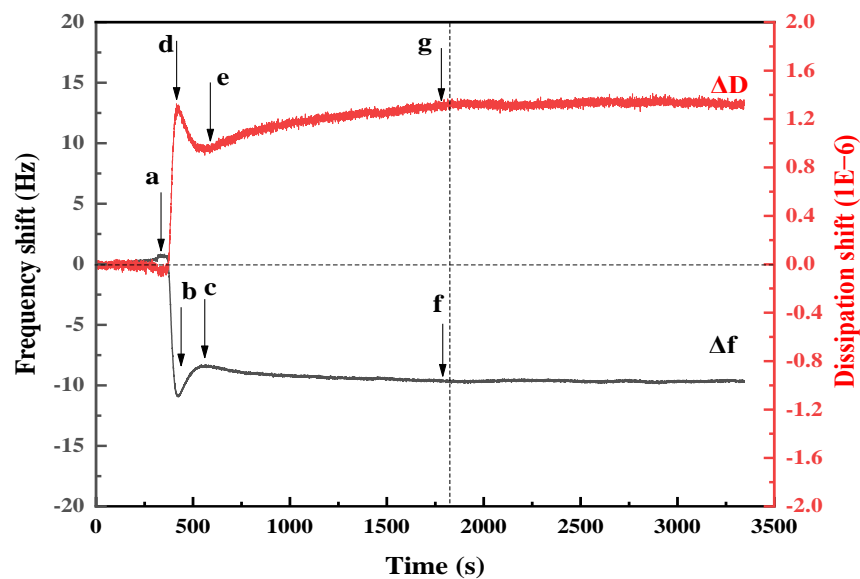


Fig. 9. Variation of frequency shift (Δf) and energy dissipation shift (ΔD) over time during the adsorption of collector GSWF01 on dolomite surface

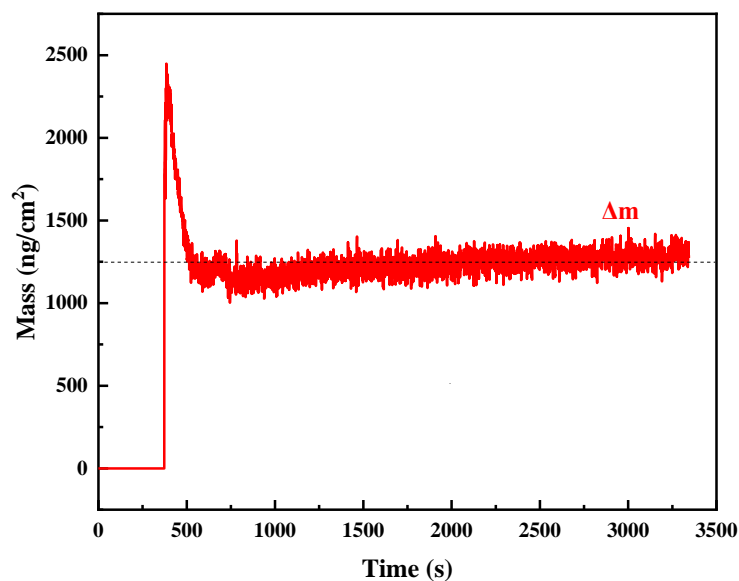


Fig. 10. Change of adsorbed layer mass of GSWF01 on dolomite surface over time

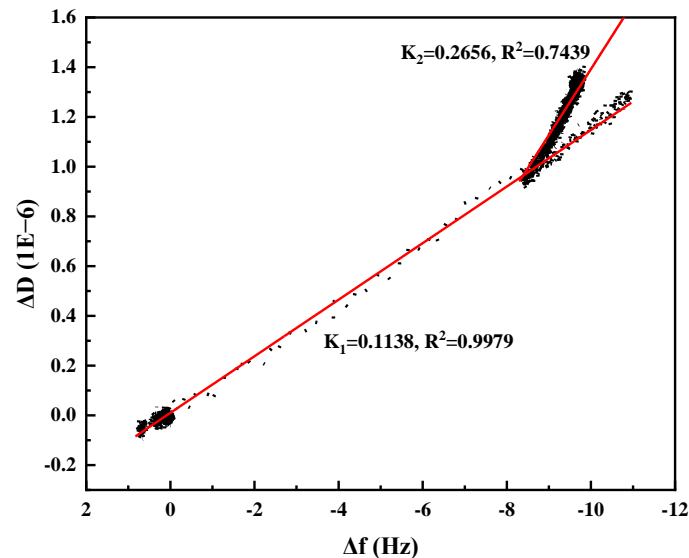


Fig. 11. ΔD - Δf plot of adsorption of GSWF01 on dolomite surface

The ΔD - Δf plot of GSWF01 adsorption was obtained by reprocessing Δf and ΔD data (Fig. 11), which can provide information on the energy dissipation per unit mass added to the probe. A straight line fitted the curves of different trends in ΔD - Δf plot, and the slope K ($K = |\Delta D/\Delta f|$) was obtained, which is an indicator for kinetic and conformation change of the adsorption process. When K value is relatively small, the system energy dissipation caused by unit adsorption capacity is small, and the adsorbed layer with firm adsorption and tight arrangement is generated. When K value is large, the adsorbed layer has high viscoelasticity and a loose structure. If there is only one K , the adsorbed layer's structure does not change during the adsorption process. More than one K indicates that a multilayer structure appears in the adsorption process or that the arrangement direction of molecules adsorbed on the surface has changed (Paul et al. 2008; Kou et al. 2015).

As shown in Fig. 11, GSWF01 adsorption on the dolomite surface had gone through two stages, with two K values obtained ($K_1 = 0.1138$, $K_2 = 0.2656$). Kou et al. (2010) showed that if $K_1 < 0.2$ and $K_2 > 0.2$, a solid monolayer with low adsorption capacity was formed first during GSWF01 adsorption on dolomite surface, and with the increase of adsorption capacity and the coupling effect of water molecules, an adsorption layer with a loose structure and high energy dissipation was gradually formed.

3.2.2. AFM analysis

AFM scanning was performed on the surface of the fresh dolomite-coated resonator and the dolomite surface after the QCM-D adsorption test to better understand the morphological changes of the dolomite surface before and after adsorption of collector GSWF01, as shown in Fig. 12. Fig. 12a displays that the dolomite-coated surface height difference was minimal (the root mean square roughness (R_q) and average roughness (R_a) were 1.366 nm and 1.040 nm, respectively), providing a relatively homogeneous and smooth dolomite-coated surface for adsorption. As Fig. 12b displays, once GSWF01 was adsorbed on the dolomite surface, the original uniform structure was barely visible, showing the existence of the adsorption layer, which was locally peak-like, with a greater height difference (R_q and R_a values were 2.452 nm and 1.748 nm, respectively). The red box area in the Fig. 12b, in particular, had a thick adsorption layer and obvious agglomeration characteristics, which may be caused by the precipitation and aggregation of fatty acid metal salts on the dolomite surface (Paiva et al. 2011). This was basically consistent with the adsorption characteristics of QCM-D.

3.2.3. IR analysis

In order to further verify the adsorption form of GSWF01 on the dolomite surface, the infrared spectra before and after interaction with GSWF01 were characterized respectively, as shown in Fig. 13. In the

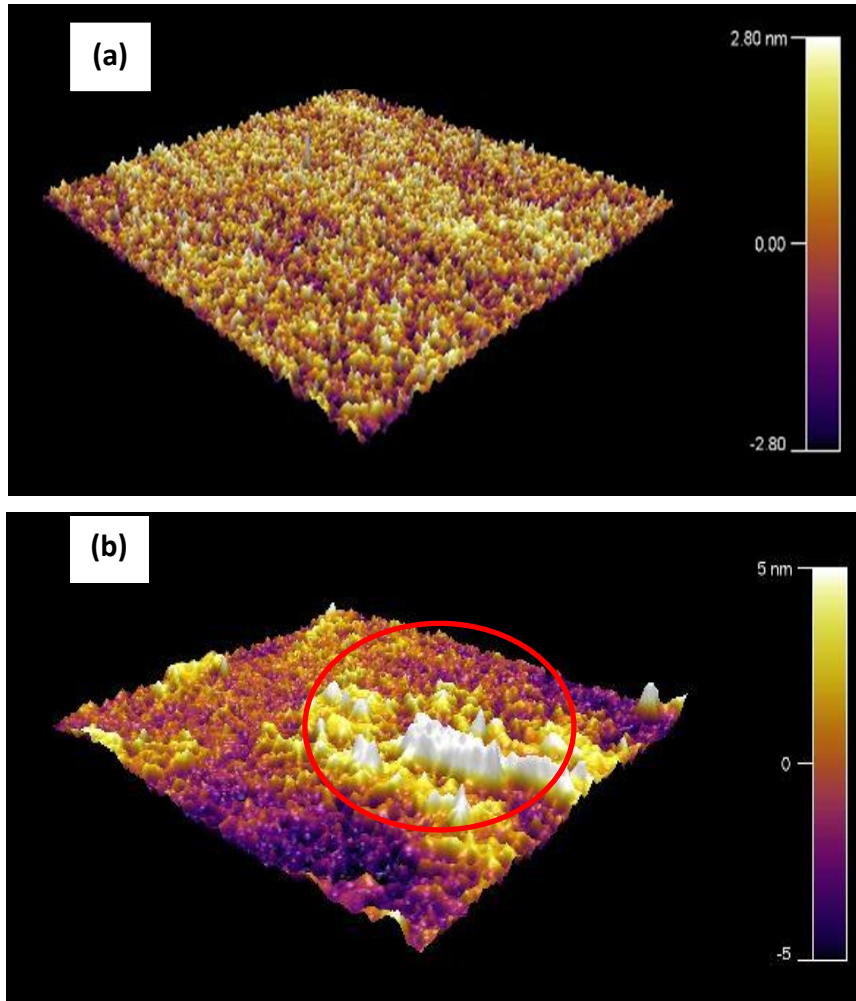


Fig. 12. AFM scanning images of dolomite surface before and after interaction with collector GSWF01: (a) 3D morphology of dolomite surface ; (b) 3D morphology of dolomite surface adsorbed by GSWF01

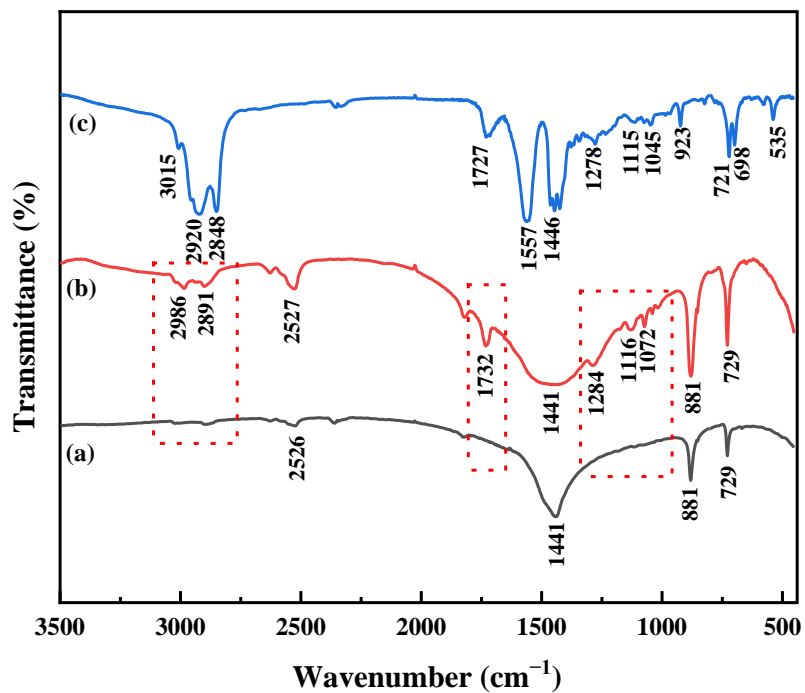


Fig. 13. Infrared spectra of dolomite (a), dolomite adsorbed with GSWF01 (b), and GSWF01 (c)

infrared spectrogram of dolomite (Fig. 13a), the CO_3^{2-} ion anti-symmetric stretching vibration absorption peak at 1441 cm^{-1} , CO_3^{2-} ion out-of-plane bending vibration absorption peak at 881 cm^{-1} , and CO_3^{2-} ion in-plane bending vibration absorption peak at 729 cm^{-1} were all characteristic absorption peaks of dolomite (Weng 2010). The C-H stretching vibration absorption peak in unsaturated C=C bond, asymmetric stretching vibration absorption peak of $-\text{CH}_2-$, and the symmetric stretching vibration absorption peak of $-\text{CH}_2-$ were 3015 cm^{-1} , 2920 cm^{-1} , and 2848 cm^{-1} in the infrared spectrogram of GSWF01 (Fig. 13c), respectively. The C=O stretching vibration absorption peak, COO- anti-symmetric stretching vibration absorption peak, and COO- symmetric stretching vibration absorption peak were 1727 cm^{-1} , 1557 cm^{-1} , and 1446 cm^{-1} , respectively. The out-of-plane bending vibration absorption peak of $-\text{COOH}$, plane rocking vibration absorption peak of $-\text{CH}_2-$, and in-plane bending vibration absorption peak of $-\text{C}-\text{C}=\text{O}$ were 923 cm^{-1} , 721 cm^{-1} , and 535 cm^{-1} , respectively. These were the characteristic absorption peaks of the fatty acid soap collector, GSWF01. After the interaction of GSWF01 with dolomite, anti-symmetric stretching vibration absorption peak and symmetric stretching vibration absorption peak of $-\text{CH}_2-$ appeared at 2986 cm^{-1} and 2891 cm^{-1} , respectively, with a blue shift, as shown in Fig. 13b. The stretching vibration absorption peak of C=O in COO- also appeared at 1732 cm^{-1} , and some weak absorption peaks consistent with GSWF01 also appeared in the fingerprint region. After GSWF01 treatment, a new characteristic absorption peak and wave peak movement appeared in the infrared spectrum of dolomite, indicating chemical adsorption between GSWF01 and dolomite. This was consistent with the findings of Hu and Wang (1990), as well as previous QCM-D and AFM results, indicating that GSWF01 adsorption on the dolomite surface was due to the formation of fatty acid metal salt precipitation by surface chemical reaction, which enhanced the hydrophobicity of the dolomite surface.

3.2.4. Zeta potential measurements

The variation of zeta potential before and after the interaction of dolomite and GSWF01 at different pH values is shown in Fig. 14. At the same pH value, the zeta potential of dolomite shifted negatively after the addition of GSWF01. The potential reduction range was the greatest at weak acidic conditions (pH = 5), and the mineral adsorption capacity was the strongest, which was consistent with the flotation practice effect of the previously selected ore. The above results showed that the fatty acid radicals with the same charge as the mineral surface were well adsorbed on the mineral surface, which can be considered as fatty acid radical ions adsorption on the surface of the mineral Helmholtz layer ((Mehdilo et al. 2013), and the interaction between fatty acid radical and dolomite was primarily chemical action rather than electrostatic force. This was consistent with the findings of Liu et al. (2016) in their study of the chemical properties of sodium oleate solution. When the pH value is 4-8, the dominant groups of sodium fatty acid solution are RCOO^- and $(\text{RCOO})_2^{2-}$, which chemically react with

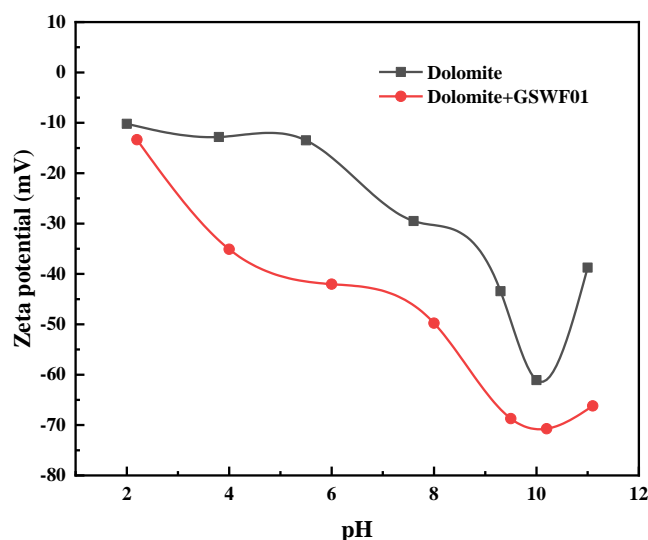


Fig. 14. Relationship between pH and zeta potential of dolomite before and after collector adsorption (collector concentration, 6 mmol/dm^3)

the active sites on the dolomite surface (e.g., Ca^{2+} , Mg^{2+} , CaOH^+ , MgOH^+) to generate surface fatty acid salt precipitates, making the dolomite surface hydrophobic and easy to float upward. The above infrared spectroscopic analysis also had further proved this point. Furthermore, there is a certain amount of RCOOH (aq) and ion-molecular association compounds ($\text{RCOOH} \cdot \text{RCOO}^-$) in a weak acidic solution environment and physical adsorption (electrostatic force and van der Waals force) between them and dolomite may also exist. According to Wang and Hu (1998), the hydrocarbon chain of $\text{RCOOH} \cdot \text{RCOO}^-$ is doubled compared to a single ion. $\text{RCOOH} \cdot \text{RCOO}^-$ has greater surface activity when the polar group is the same. Therefore, in addition to RCOOH (aq), $(\text{RCOO})_2^{2-}$ and RCOO^- , the ion-molecular association compounds $\text{RCOOH} \cdot \text{RCOO}^-$ may also play a certain role in determining the hydrophobic floating of dolomite.

4. Conclusions

The microscopic mechanism of interface adsorption between collector (GSWF01) and mineral (dolomite) was explored using the flotation practice of carbonate phosphate ore, and the following conclusions can be drawn:

(1) The selected phosphate ore used was fine-grained dolomitic collophanite with a high P_2O_5 grade (27.67%), with dolomite as the major gangue mineral. On the selected ore, a single reverse flotation test with different pH and collector dosage was carried out using a novel mixed fatty acid soap (GSWF01) as dolomite collector and acidic industrial wastewater (WFS) as pH regulator and inhibitor. A phosphate concentrate with P_2O_5 grade of 33.73%, MgO content of 1.07%, MER value ($\omega(\text{MgO}+\text{Al}_2\text{O}_3+\text{Fe}_2\text{O}_3)/\omega(\text{P}_2\text{O}_5)$) of 4.86%, MgO removal of 83.86% and phosphorus recovery of 91.06% was obtained, which can be used as a high-quality raw material for downstream wet-process phosphoric acid production. Multi-component GSWF01 is more suitable for the complex flotation system of dolomitic collophanite than NaOL.

(2) The interaction between GSWF01 and dolomite was mainly chemical adsorption, which was the reaction of fatty acid radicals (RCOO^- and $(\text{RCOO})_2^{2-}$) with surface metal ions (Ca^{2+} , Mg^{2+} , etc.) to form fatty acid salt precipitation. The adsorption occurred in two stages, and two K values were obtained with $K_1 < 0.2$ and $K_2 > 0.2$, indicating that during the adsorption process, a solid monolayer with low adsorption capacity was formed first, and then an adsorbed layer with a loose structure and high energy dissipation was gradually formed with the increase in adsorption capacity and the coupling effect of water molecules. This is the main reason for the hydrophobic floating of dolomite. Moreover, in a weak acidic solution environment, physical adsorption of fatty acid molecules (RCOOH (aq)) and fatty acid ion-molecular association compounds ($\text{RCOOH} \cdot \text{RCOO}^-$) generated by hydrolysis can also occur on the dolomite surface.

(3) In summary, several factors influence the adsorption performance between minerals and reagents in the practice of phosphate ore flotation engineering, including pulp solution pH, the type and dosage of collectors and inhibitors, as well as mineral particle size, separation process, and equipment. However, controlling the physical and chemical properties of the solution by strengthening the combination of collectors or inhibitors remains a key technique to achieve efficient flotation separation of minerals.

Acknowledgments

This research was sponsored by National Natural Science Foundation of China (51874221), Open Foundation of State Key Laboratory of Mineral Processing (BGRIMM-KJSKL-2021-08), and Science and Technology Program of Guizhou Province (Qiankehe support (2020) 2Y048).

References

- CAO, Q.B., CHENG, J. H., WEN, S. M., LI, C. X., BAI, S. J., LIU, D., 2015. *A mixed collector system for phosphate flotation*. Minerals Engineering, 78, 114-121.
- DENG, J., ZHANG, K. C., HE, D. S., ZHAO, H. Q., HAKKOU, R., BENZAAZOUA, M., 2020. *Occurrence of sesquioxide in a mid-low grade collophane-sedimentary apatite ore from Guizhou, China*. Minerals, 10, 1038.

- DENG, M. J., LIU, Q. X., XU, Z. H., 2013. *Impact of gypsum supersaturated solution on surface properties of silica and sphalerite minerals*. Minerals Engineering, 47, 6-15.
- DERHY, M., YASSINE, T., HAKKOU, R., BENZAAZOUA, M., 2020. *Review of the main factors affecting the flotation of phosphate ores*. Minerals, 10, 1109.
- GUTIG, C., GRADY B. P., STRIOLO, A., 2008. *Experimental studies on the adsorption of two surfactants on solid-aqueous interfaces: Adsorption isotherms and kinetics*. Langmuir, 24, 4806-4816.
- HU, Y. H., WANG, D. Z., 1990. *Mechanism of fatty acid sodium flotation of salt-type minerals – a study*. Mining and Metallurgical Engineering, 10, 20-23.
- KOU, J., TAO, D., XU, G., 2010a. *A study of adsorption of dodecylamine on quartz surface using quartz crystal microbalance with dissipation*. Colloids and Surfaces A: Physicochemical and Engineering Aspects, 368, 75-83.
- KOU, J., TAO, D., XU, G., 2010b. *Fatty acid collectors for phosphate flotation and their adsorption behavior using QCM-D*. International Journal of Mineral Processing, 95, 1-9.
- KOU, J., XU, S., SUN, T., SUN, C., GUO, Y., WANG, C., 2016. *A study of sodium oleate adsorption on Ca²⁺ activated quartz surface using quartz crystal microbalance with dissipation*. International Journal of Mineral Processing, 154, 24-34.
- KOU, J., GUO, Y., SUN, T. C., XU, S. H., XU, C. Y., 2015. *Adsorption mechanism of two different anionic collectors on quartz surface*. Journal of Central South University (Science and Technology), 46, 4005-4014.
- LI, F., TIAN, P. J., 2016. *Research on reverse flotation test and mechanism of a siliceous collophanite*. Industrial Minerals & Processing, 45, 8-10.
- LIU, C., FENG, Q. M., ZHANG, G. F., 2016. *Flotation behaviors and mechanism of hemimorphit using sodium oleate as collector*. The Chinese Journal of Nonferrous Metals, 26, 878-883.
- LIU, X., LI, C. X., LUO, H. H., CHENG, R. J., LIU, F. Y., 2017. *Selective reverse flotation of apatite from dolomite in collophanite ore using saponified gutter oil fatty acid as a collector*. International Journal of Mineral Processing, 165, 20-27.
- LIU, X., LUO, H. H., CHENG, R. J., LI, C. X., ZHANG, J. H., 2017a. *Effect of citric acid and flotation performance of combined depressant on collophanite ore*. Minerals Engineering, 109, 162-168.
- LIU, X., RUAN, Y. Y., LI, C. X., CHENG, R. J., 2017b. *Effect and mechanism of phosphoric acid in the apatite/dolomite flotation system*. International Journal of Mineral Processing, 167, 95-102.
- MEHDILO, A., IRANNAJAD, M., REZAI, B., 2013. *Effect of chemical composition and crystal chemistry on the zeta potential of ilmenite*. Colloids and Surfaces A: Physicochemical and Engineering Aspects, 428, 111-119.
- PAIVA, P. R. P., MONTE, M. B. M., SIMAO, R. A., GASPAS, J. C., 2011. *In situ AFM study of potassium oleate adsorption and calcium precipitate formation on an apatite surface*. Minerals Engineering, 24, 387-395.
- PAUL, S., PAUL, D., BASOVA, T., RAY, A. K., 2008. *Studies of adsorption and viscoelastic properties of proteins onto liquid crystal phthalocyanine surface using quartz crystal microbalance with dissipation technique*. The Journal of Physical Chemistry C, 112, 11822-11830.
- QI, Z., SUN, C. Y., 2013. *Study of flotation behavior and mechanism of dolomite with fatty acid as collector*. Journal of China University of Mining & Technology, 42, 461-465.
- RUAN, Y. Y., HE, D. S., CHI, R. A., 2019. *Review on beneficiation techniques and reagents used for phosphate ores*. Minerals, 9, 253.
- RUAN, Y. Y., ZHANG, Z. Q., LUO, H. H., XIAO, C. Q., ZHOU, F., CHI, R. A., 2017. *Ambient temperature flotation of sedimentary phosphate ore using cottonseed oil as a collector*. Minerals, 7, 65.
- RUAN, Y. Y., ZHANG, Z. Q., LUO, H. H., XIAO, C. Q., ZHOU, F., CHI, R. A., 2018. *Effects of metal ions on the flotation of apatite, dolomite and quartz*. Minerals, 8, 141.
- SAUERBREY, G., 1959. *Verwendung von schwingquarzen zur wägung dünner schichten und zur mikrowägung*. Zeitschrift für Physik, 155, 206-222.
- SEDEVA, I. G., FETZER, R., FOMASIERO D., RALSTON, J., BEATTIE, D. A., 2010. *Adsorption of modified dextrans to a hydrophobic surface: QCM-D studies, AFM imaging, and dynamic contact angle measurements*. Journal of Colloid and Interface Science, 345, 417-426.
- SHI, B., XU, W., TIAN, Y., CHEN, Y., ZHAO, Y. Y., CHENG, Q., MEI, G. J., 2021. *Study on reverse flotation of a calcium-magnesium phosphate rock in Guizhou using collector WF-04 and its function*. Industrial Minerals & Processing, 50, 10-13.

- TENG, F. C., LIU, Q. X., ZENG, H. B., 2012. *In situ kinetic study of zinc sulfide activation using a quartz crystal microbalance with dissipation (QCM-D)*. Journal of Colloid and Interface Science, 368, 512-520.
- VOGT, B. D., LIN, E. K., WU, W. L., WHITE, C. C., 2004. *Effect of film thickness on the validity of the sauerbrey equation for hydrated polyelectrolyte films*. The Journal of Physical Chemistry B, 108, 12685-12690.
- VOINOVA, M.V., RODAHL, M., JONSON, M., KASEMO, B., 1998. *Viscoelastic acoustic response of layered polymer films at fluid-solid interfaces: Continuum mechanics approach*. Physica Scripta, 59, 391-396.
- WANG, D. Z., HU, Y. H., 1998. *Flotation Solution Chemistry*. Hunan science & technology press, Changsha, China.
- WENG, S. F., 2010. *FTIR Spectral Analysis*. Chemical Industry Pres, Beijing, China.
- XU, W., SHI, B., TIAN, Y., CHEN, Y., LI, S. Q., CHENG, Q., MEI, G. J., 2021. *Process mineralogy characteristics and flotation application of a refractory colophonite from Guizhou, China*. Minerals, 11, 1249.
- XU, W., LAN, F., YANG, S., HU, D. Y., ZHANG, R. Z., CHEN, Y., XIE, T., 2012. *Study on reverse-flotation test of the new combined collector LG-01 for a carbonate phosphate from Guizhou*. Metal Mine, 41, 99-101.
- YU, J., GE, Y. Y., GUO, X. L., GUO, W. B., 2016. *The depression effect and mechanism of NSFC on dolomite in the flotation of phosphate ore*. Separation and Purification Technology, 161, 88-95.
- ZOU, H., CAO, Q. B., LIU, D. W., YU, X. C., LAI, H., 2019. *Surface features of fluoroapatite and dolomite in the reverse flotation process using sulfuric acid as a depressor*. Minerals, 9, 33.